2021 International Conference on Unmanned Aircraft Systems (ICUAS)
Athens, Greece. June 15-18, 2021

Curvature-Constrained Vector Field for Path Following Guidance

Amit Shivam
Department of Aerospace Engineering
Indian Institute of Science
Bangalore, India
amitshivam@iisc.ac.in

Ashwini Ratnoo
Department of Aerospace Engineering
Indian Institute of Science
Bangalore, India
ratnoo@iisc.ac.in

2021 International Conference on Unmanned Aircraft Systems (ICUAS) | 978-1-6654-1535-4/21/$31.00 ©2021 IEEE | DOI: 10.1109/ICUAS51884.2021.9476741

***Abstract*—This paper introduces a new vector field guidance method to generate continuously flyable paths for unmanned air vehicles. The central idea of the proposed vector field approach is imbibed in the commanded course angle, which is expressed as a nonlinear function of the position error with respect to the desired path. Considering straight line and circular paths, the asymptotic behavior of position error is shown to converge to zero. Analysis of path curvature establishes a significantly lower maximum value as compared to a popular existing method. Simulation results are presented considering a two-dimensional kinematic model of the vehicle. Overall, the method presents an easily computable path following solution with superior curvature characteristics.**

***Index Terms*—Path Planning**

I. Introduction

Applications of Unmanned Air Vehicles (UAVs) have increased rapidly in recent decades, encompassing defense, agriculture, healthcare, and various civilian aspects. These missions often require a UAV to follow predefined paths autonomously. Algorithms used for generating path following guidance command should be low in complexity, accurate in performance, issue commands within the vehicle's dynamic capability.

The existing literature on path following guidance problem can be broadly categorized as virtual target-based approaches, control theory-based solutions, and vector field-based methods. The virtual target-based framework utilizes classical missile guidance laws like a pure pursuit [1], line-of-sight guidance [2], proportional navigation and its variants [3], [4]. The guidance law directs a UAV to follow a virtual target moving at a fixed look-ahead distance on the desired path which eventually drives the UAV to the path. One of the concerns with this class of solutions is the lack of virtual target existence guarantee in case there are significant disturbances that increase the UAV relative separation beyond the prescribed look-ahead distance.

Several types of control design techniques have been developed for path-following problems in robotics that include various class of UAVs. Ref. [5], presents a survey of path following algorithms including methods like linear quadratic regulator (LQR), sliding mode control, model predictive control, back-stepping control, and adaptive control. An adaptive optimal UAV guidance law using linear quadratic regulator (LQR) formulation is presented for tighter control on errors in the presence of high wind disturbances in [6]. Ref. [7] uses the optimal guidance for achieving terminal impact angle against a target for developing path following guidance logic. In [8], sliding mode control design is used to follow commanded course angle, thereby leading the UAV to the desired straight line or circular path. Ref. [9] proposes model predictive control to compute commanded heading direction for tracking of boundaries. Back-stepping controller design is used for underactuated follower-UAV equipped with pan-tilt camera to achieve the objective of following leader-UAV autonomously in [10].

Vector fields present a novel path following approach which fuses both the path planning and path tracking elements into one. By providing a commanded heading direction at each point in the workspace, vector fields provide guidance inputs that are robust to disturbances, obstacle avoiding deviations and other realistic perturbations. Vector field based commanded course angle guidance for straight line and circular orbit is discussed in Ref. [8,11,12]. Nelson et al. [8,11] introduced vector fields approach wherein the tangent of the commanded course angle at a location was proportional to the positional error with respect to the desired path. Ref. [12], considers the lateral-error rate as a function of ground speed and relative course orientation error which is reduced to zero subsequently using the method presented in [8]. Stable course angle variation is not inherently guaranteed for these vector fields and Lyapunov's direct approach was used to prove the same.

Lyapunov vector field utilizes the property of positive definite potential function to construct a stable vector field. The basic construction consists of a contraction term that governs the radial speed and a circulation term which controls the tangential speed with respect to the reference point or path. This approach is realized extensively in coordinated standoff target tracking scenario for stationary [13], and maneuvering [14], [15], [16] target. Lim et al. [15], presented a numerical integration method for calculating individual UAV paths to achieve simultaneous stand-off tracking of target at desired position and time, whereas, [16] proposed a modified Lyapunov vector field that provides lower maximum curvature

Authorized licensed use limited to: Technische Hochschule Ingolstadt. Downloaded on April 21,2022 at 10:30:10 UTC from IEEE Xplore. Restrictions apply.

limit while circumnavigating around a stationary target.

In most of the path following methods, the focus is on deducing smooth convergence to the path and curvature variation along the trajectory has not received significant attention. Curvature relates directly to the turning rate capability of the UAV and is hence an important consideration in UAV path following guidance algorithm design. In this work, a new vector field based guidance method is proposed for UAVs to follow desired straight line and circular paths. More versatile form of commanded course angle is proposed while considering curvature analysis to establish the significance of the proposed vector field method. As the main contributions of this work, a significant curvature advantage is established for the proposed method.

II. Proposed Guidance Law

This section discusses the proposed guidance method for the path following problem. Considering straight line and circular orbit as two desired path following scenario commanded course angle is proposed in terms of the UAV position error with respect to the path. The nonlinear kinematics of UAV for a two-dimensional engagement scenario can be expressed as

$$\dot{x} = V\cos\chi \tag{1}$$
$$\dot{y} = V\sin\chi \tag{2}$$

where, (x, y) is the instantaneous position of UAV in cartesian coordinates. Here, χ, as mentioned above is the course angle measured with respect to the positive x-axis.

A. Straight line path following

The proposed vector field guidance law considers a straight line path following scenario as shown in Fig. 1, wherein, UAV is at a distance x from the path to be followed, the desired course angle χ_d can be expressed as,

$$\chi_d = \begin{cases} \sin^{-1}\left(\frac{1}{1+k_l x^2}\right), & \text{if } x \leq 0 \\ \pi - \sin^{-1}\left(\frac{1}{1+k_l x^2}\right), & \text{otherwise} \end{cases} \tag{3}$$

where k_l is a positive constant given for straight line path following. Fig. 2 shows the proposed heading angle profile with respect to lateral error considering $k_l = 0.005$. It can be seen that the proposed course angle varies smoothly to the desired course angle on the path, that is, $\chi = \frac{\pi}{2}$ at $x = 0$. At very large distances from the path, the commanded heading is pointed along the shortest distance approach to the path, that is, $\chi = 0$ or π. The specific choice of course angle variation is motivated by the resulting curvature characteristics, more details of which will be discussed in Section III. The commanded heading variation with different choices of k_l is plotted in Fig. 3. It is evident from Fig. 3 that higher values of k_l correspond to steeper variation in course angle near the desired path.

The asymptotic behavior of proposed straight line path following guidance law can be verified using Lyapunov's indirect method. Consider a candidate Lyapunov function $W = \frac{1}{2}x^2$, which on differentiating with respect to time results in

$$\dot{W} = x\dot{x} \tag{4}$$

Using Eq. (1) and Eq. (3), in Eq. (4),

$$\dot{W} = \begin{cases} xV\cos\left(\sin^{-1}\left(\frac{1}{1+k_l x^2}\right)\right), & \text{if } x \leq 0 \\ xV\cos\left(\pi - \sin^{-1}\left(\frac{1}{1+k_l x^2}\right)\right), & \text{otherwise} \end{cases} \tag{5}$$

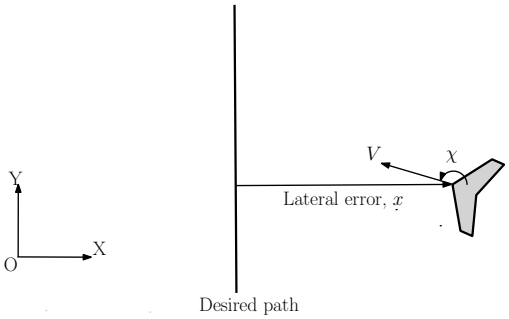

Fig. 1: Straight line path following geometry

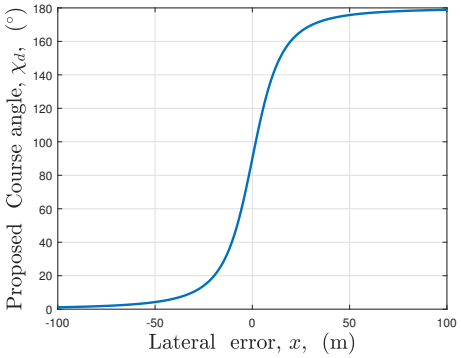

Fig. 2: Heading angle with $k_l = 0.005$

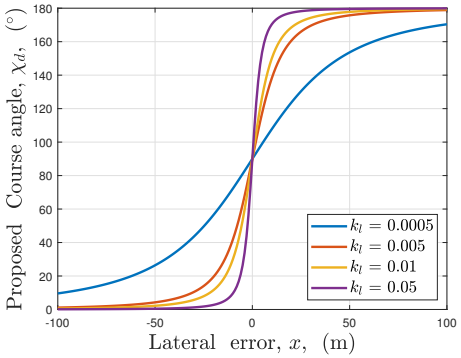

Fig. 3: Heading angle with different k_l

Authorized licensed use limited to: Technische Hochschule Ingolstadt. Downloaded on April 21,2022 at 10:30:10 UTC from IEEE Xplore. Restrictions apply.

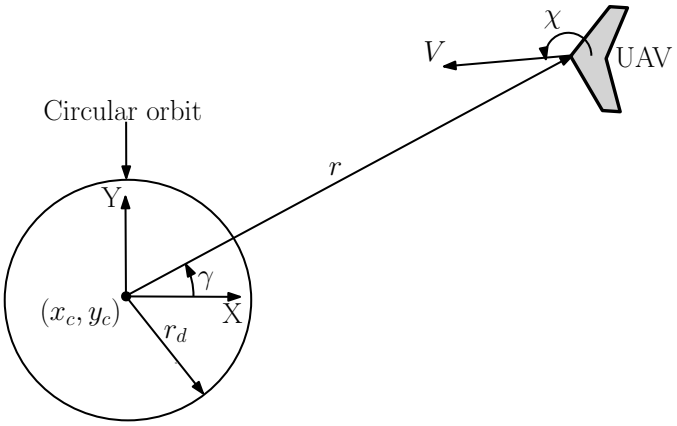

Fig. 4: Circular path following geometry

On rearranging Eqn. (5),

$$\dot{W} = -|x|\, V \cos\left(\sin^{-1}\left(\frac{1}{1+k_l x^2}\right)\right) \quad (6)$$

$$\Rightarrow \dot{W} < 0 \text{ for all } x \neq 0 \quad (7)$$

$$\text{and, } \dot{W} = 0 \text{ for } x = 0 \quad (8)$$

and hence by Lyapunov's method of stability, the lateral error converges to zero asymptotically.

B. Circular path following

Consider a circular path following scenario shown in Fig. 4, where UAV is placed outside a desired circular orbit, and instantaneous pose is represented in terms of polar coordinates (r, γ). In this case, the commanded course angle χ_d is proposed in terms of radial distance r, measured from center (x_c, y_c) of the desired circular orbit of radius r_d as

$$\chi_d = \begin{cases} \gamma + \sin^{-1}\left(\frac{1}{1+k_c(r-r_d)^2}\right), & \text{if } 0 < r \leq r_d \\ \gamma + \pi - \sin^{-1}\left(\frac{1}{1+k_c(r-r_d)^2}\right), & r \geq r_d \end{cases} \quad (9)$$

where, k_c is a positive constant for circular path following scenario. The first term in Eq. (9) corresponds to a commanded course angle variation with $\chi_d = \gamma + \frac{\pi}{2}$ at $r = r_d$. For second term in Eq. (9), the proposed course angle is directed towards the center of circular orbit for $r >> r_d$ with $\chi_d \approx \gamma + \pi$ and it attains $\chi_d = \gamma + \frac{\pi}{2}$ at $r = r_d$. The equations of motion of UAV can be expressed in polar coordinates as

$$\dot{r} = V\cos(\chi - \gamma) \quad (10)$$

$$\dot{\gamma} = \frac{V}{r}\sin(\chi - \gamma) \quad (11)$$

Similar to the analysis presented in Section A, we consider a Lyapunov function as $W = \frac{1}{2}\tilde{r}^2$, where radial distance error is expressed as $\tilde{r} = r - r_d$. Upon differentiation of the function,

$$\dot{W} = \tilde{r}\dot{\tilde{r}} \quad (12)$$

Using Eq. (10), in Eq. (12) results in

$$\dot{W} = \tilde{r}V\cos(\chi_d - \gamma) \quad (13)$$

Using Eq. (9) in Eq. (13) and on further simplification

$$\dot{W} = -|\tilde{r}|\, V \cos\left(\sin^{-1}\left(\frac{1}{1+k_c(r-r_d)^2}\right)\right) \quad (14)$$

$$\Rightarrow \dot{W} < 0 \text{ for all } r \neq r_d \quad (15)$$

$$\text{and, } \dot{W} = 0 \text{ for } r = r_d \quad (16)$$

Hence, the system is asymptotically stable about $r = r_d$.

III. Curvature characteristics

Curvature variation for the proposed vector field can be obtained as

$$\kappa = \frac{d\chi_d}{ds} = \frac{\frac{d\chi_d}{dt}}{\frac{ds}{dt}} = \frac{\dot{\chi}_d}{V} \quad (17)$$

From Eq. (17), it is clear that curvature is directly proportional to turn rate of UAV.

A. Straight line path

Using Eq. (3) and considering $x > 0$, the course rate can be obtained as

$$\dot{\chi}_d = \frac{2k_l x}{(1+k_l x^2)\sqrt{k_l^2 x^4 + 2k_l x^2}}\dot{x} \quad (18)$$

Using Eq. (1) and Eq. (3), in Eq. (18)

$$\dot{\chi}_d = \frac{2k_l x}{(1+k_l x^2)\sqrt{k_l^2 x^4 + 2k_l x^2}} V\cos\chi_d \quad (19)$$

On further simplifying and rearranging Eq. (19)

$$\dot{\chi}_d = -\frac{2Vk_l x}{(1+k_l x^2)^2} \quad (20)$$

Finally, using Eq. (17), an expression for the curvature can be deduced as

$$\kappa = -\frac{2k_l x}{(1+k_l x^2)^2} \quad (21)$$

The curvature maxima can be obtained on solving $\frac{d\kappa}{dx} = 0$. Accordingly,

$$\frac{d}{dx}\left\{\frac{-2k_l x}{(1+k_l x^2)^2}\right\} = 0, \;\Rightarrow x = \frac{1}{\sqrt{3k_l}} \quad (22)$$

Using Eq. (22) in Eq. (21), the maximum curvature can be obtained as $\kappa_{max} = \frac{-9}{8}\sqrt{\frac{k_l}{3}}$, which occurs at $x = \frac{1}{\sqrt{3k_l}}$.

B. Circular path

Similar to the case of straight lines, the expression of curvature for the circular path can be obtained by using Eq. (17) as

$$\kappa = \frac{1}{r\left(1+k_c(r-r_d)^2\right)} - \frac{2k_c(r-r_d)}{\left(1+k_c(r-r_d)^2\right)^2} \text{ for all } r \geq r_d \quad (23)$$

On differentiating Eq. (23), w.r.t r, a higher-order nonlinear equation is obtained, which does not lead to feasible explicit closed-form expression of maximum curvature.

Authorized licensed use limited to: Technische Hochschule Ingolstadt. Downloaded on April 21,2022 at 10:30:10 UTC from IEEE Xplore. Restrictions apply.

IV. Simulation and Results

This section considers a two-dimensional kinematic model for simulation studies with first order course control. The first order course control considered for simulation results can be expressed as

$$\dot{\chi} = \alpha\,(\chi_d - \chi) \tag{24}$$

where, α is a proportional gain constant. Considering straight line and circular path following scenario, UAV trajectory and corresponding parameters establishing successful convergence across the desired trajectory are plotted in subsequent sections.

A. Straight line path following

Consider an initial position of UAV at $(x_0, y_0) = (90\text{m}, -90\text{m})$ with a constant speed of $V = 25$ m/s is assigned to follow the desired path at $x = 0$ m. The proposed vector field is generated using gain $k_l = 0.0015$ which corresponds to a commanded course direction (using Eqn. (3)) of 176.4 degree at initial lateral error(initial x-cordinates) $x_0 = 90$ m. Fig. 5a plots UAV trajectory to follow desired straight line path at $x = 0$ m. Fig. 5b shows course angle converges to 90 degree at zero lateral error, thereby leading to the desired path. Fig. 5c illustrates the convergence of lateral error to zero.

Fig. 5d demonstrate the comparative curvature performance with Nelson et al. for straight line path following scenario. The curvature maxima expression for considered commanded course angle of 176.4 degree and given initial lateral error results in $\kappa_{max} = -\frac{2.59}{x_0}$ for the proposed method, whereas, for Nelson et al., corresponding expression is $\kappa_{max} = -\frac{6.12}{x_0}$. The curvature maxima so obtained for initial lateral error of 90 m, results in $\kappa_{max} = -0.028$ m^{-1} at $x = 13.45$ m for the proposed method, which matches the theoretical value as discussed in Section III. Maximum curvature for Ref. [8], is $\kappa_{max} = -0.068$ m^{-1} at $x = 4.00$ m. The comparative results show the significant advantage of the method offers in terms of the maximum curvature of the path.

B. Circular path following

Consider a desired circular orbit of center $(x_c, y_c) = (0\text{m}, 0\text{m})$ and radius $r_d = 50$m is used for simulation studies. Here, speed of UAV is kept constant at 25 m/s and gain k_c is calculated for each case.

1) Initial point outside a circular orbit: For initial point outside the orbit, UAV is considered to be at $(r_0, \gamma_0) = (100\text{m}, 5°)$ with initial course angle $\chi_0 = 150°$ and the gain constant k_c used for simulation is 0.006. Fig. 6a shows UAV trajectory for path following of circular orbit. Fig. 6b illustrates radial error converges to zero in approximately 4 seconds. The corresponding radial distance converges to the desired radius of $r_d = 50$ m as shown in Fig. 6c.

Fig. 6d illustrate the comparative curvature performance with Nelson et al. [8]. The curvature maxima for the proposed method results in $\kappa_{max} = -0.038$ m^{-1} at $r = 58.36$ m, whereas, that for Ref. [8], maximum curvature is $\kappa_{max} = -0.107$ m^{-1} at $r = 52.31$ m.

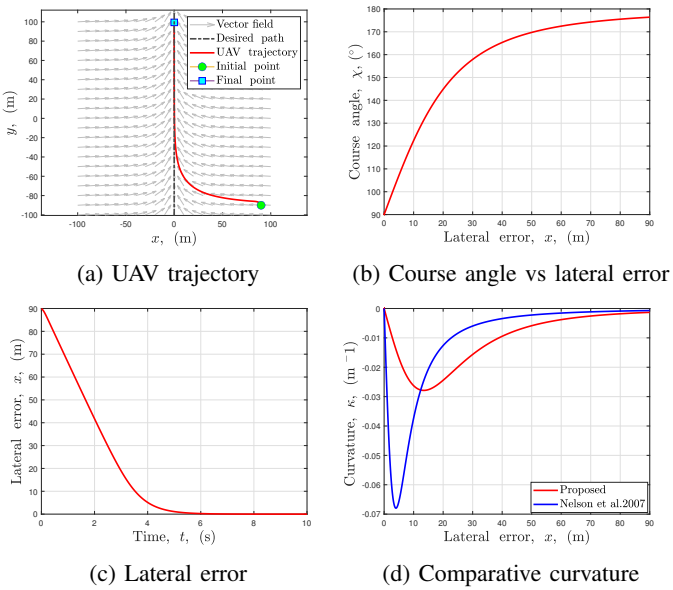

(a) UAV trajectory (b) Course angle vs lateral error

(c) Lateral error (d) Comparative curvature

Fig. 5: Results for Case A with $x_0 = 90$ m and $\alpha = 50$

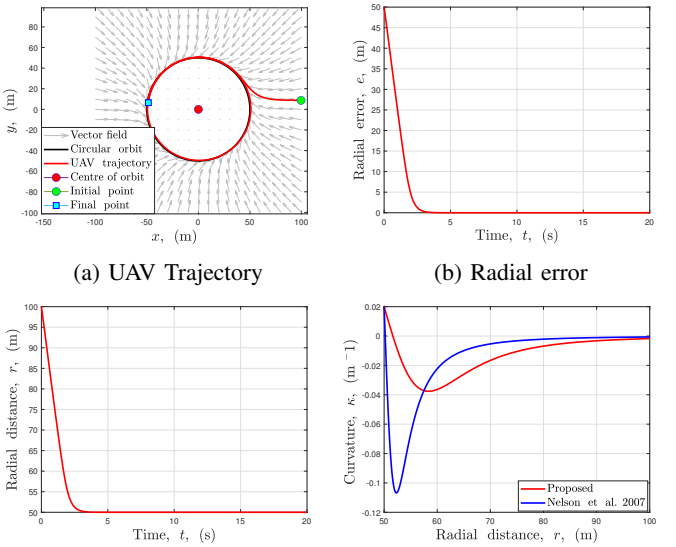

(a) UAV Trajectory (b) Radial error

(c) Radial distance (d) Comparative curvature profile

Fig. 6: Results for Case B with initial point outside a circular orbit at $r_0 = 100$ m and proportional gain $\alpha = 50$

2) Initial point inside a circular orbit: UAV is considered to be inside a circular orbit at $(r_0, \gamma_0) = (10\text{m}, 5°)$ with initial course angle $\chi_0 = 30°$, while considering the desired orbit radius to be the same as in Case 1. The gain constant k_c is considered to be 0.009 for this case. Fig. 7a represents the trajectory of UAV. Fig. 7b illustrates that the radial error converges to zero in approximately 3 seconds. Fig. 7c illustrates successful convergence to a desired circular orbit.

Fig. 7d demonstrate the comparative curvature performance with Ref. [8]. The maximum curvature for the proposed method resulted in $\kappa_{max} = 0.08$ m^{-1}, which occurs at

Authorized licensed use limited to: Technische Hochschule Ingolstadt. Downloaded on April 21,2022 at 10:30:10 UTC from IEEE Xplore. Restrictions apply.

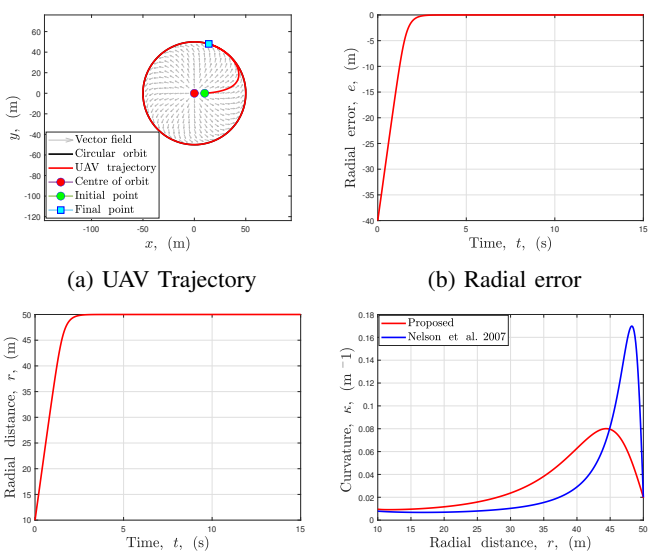

(a) UAV Trajectory (b) Radial error

(c) Radial distance (d) Comparative curvature profile

Fig. 7: Results for Case B with initial point inside a circular orbit at $r_0 = 10$ m and proportional gain $\alpha = 50$

position $r = 44.69$ m, whereas, for the method proposed in Ref. [8], maximum curvature found to be $\kappa_{max} = 0.17$ m^{-1}, at $r = 48.26$ m.

V. Conclusions

A new vector field is proposed for straight line and circular path following. The proposed vector field generates a commanded heading direction as an arc-sin variation of a nonlinear function of the position error throughout the domain of interest. Curvature analysis is carried out to obtain a closed-form expression of the maximum curvature for the straight line path following scenario. Simulation results show a significant advantage for the proposed method in terms of the maximum curvature as compared to a popular existing method. Addressing variable curvature and validation with high fidelity vehicle model are some future directions.

References

[1] E. D. B. Medagoda, and P. W. Gibbens "Synthetic-Waypoint Guidance Algorithm for Following a Desired Flight Trajectory," *Journal of Guidance, Control, and Dynamics*, Vol. 33, No. 2, April 2010, pp. 601-606.

[2] R. Rysdyk, "UAV Path Following for Constant Line-of-Sight," in *2nd AIAA "Unmanned Unlimited" Conference and Workshop Exhibit*, San Diego, California, USA, Sep. 15-18, 2003, AIAA Paper 2003-6626.

[3] M. Kothari, I. Postlethwaite, and D. W. Gu, "A Suboptimal Path Planning Algorithm Using Rapidly-Exploring Random Trees," *International Journal of Aerospace Innovations*, Vol. 2, No. 1, February 2010, pp. 93-103.

[4] S. Park, J. Deyst, and J. P. How, "Performance and Lyapunov Stability of a Nonlinear Path Following Guidance Method," *Journal of Guidance, Control, and Dynamic*, Vol. 30, No. 6, May 2012, pp. 1718-1728.

[5] P. B. Sujit, S. Saripalli, and J. B. Sousa, "Unmanned Aerial Vehicle Path Following: A Survey and Analysis of Algorithms for Fixed-Wing Unmanned Aerial Vehicles," *IEEE Control Systems Magazine*, Vol. 34, No. 1, February 2014, pp. 42-59.

[6] A. Ratnoo, P.B. Sujit, and M. Kothari, "Adaptive Optimal Path Following for High Wind Flights," *IFAC Proceedings Volumes*, Vol. 44, No. 1, January 2011, pp. 12985-12990.

[7] A. Ratnoo, Y. S. Hayoun, A. Granot, and, T. Shima, "Path following using trajectory shaping guidance," *Journal of Guidance, Control, and Dynamics*, Vol. 38, No. 1, December 2014, pp. 106-116.

[8] D. R. Nelson, D. B. Barber, T. W. McLain, and R.W. Beard, "Vector Field Path Following for Miniature Air Vehicles," *IEEE Transactions on Robotics*, Vol. 23, No. 3, June 2007, pp. 519-529.

[9] K. Patnaik, and A. Ratnoo, "Boundary Tracking Using Sampling Based Model Predictive Control Law," in *AIAA Scitech 2019 Forum*, San Diego, California, USA, Jan. 7-11, 2019, AIAA Paper 2019-1414.

[10] V. K. Chitrakaran, D. M. Dawson, H. Kannan, and M. Feemster, "Vision Assisted Autonomous Path Following for Unmanned Aerial Vehicles," in *Proc. 45th IEEE Conf. Decision Control*, Dec. 13-15, 2006, pp. 63–68.

[11] D. R. Nelson, D. B. Barber, T. W. McLain, and R.W. Beard, "Vector Field Path Following for Small Unmanned Air Vehicles," *IEEE American Control Conference*, Piscataway, NJ, June 2006, pp. 5788-5794.

[12] S. Griffiths, "Vector Field Approach for Curved Path Following for Miniature Aerial Vehicles," *AIAA Guidance, Navigation, and Control Conference Exhibit*, Keystone, Colorado, USA, Aug. 21-24, 2006, AIAA Paper 2006-6467.

[13] D. A. Lawrence, "Lyapunov Vector Fields for UAV Flock Coordination," in *2nd AIAA "Unmanned Unlimited" Conference and Workshop Exhibit*, San Diego, California, USA, Sep. 15-18, 2003, AIAA Paper 2003-6575.

[14] D. A. Lawrence, E. W. Frew, and W. J. Pisano, "Lyapunov Vector Fields for Autonomous Unmanned Aircraft Flight Control," *Journal of Guidance, Control, and Dynamics*, October 2008, Vol. 31, No. 5, pp. 1220-1229.

[15] S. Lim, Y. Kim, D. Lee, and H. Bang, "Stand-Off Target Tracking Using a Vector Field for Multiple Unmanned Aircrafts," *Journal of Intelligent and Robotic Systems*, Vol. 69, No. 1, September 2013, pp. 347-360.

[16] A. A. Pothen, and A. Ratnoo, "Curvature-Constrained Lyapunov Vector Field for Standoff Target Tracking," *Journal of Guidance, Control, and Dynamics*, Vol. 40, No. 10, June 2017, pp. 2729-2736.

Authorized licensed use limited to: Technische Hochschule Ingolstadt. Downloaded on April 21,2022 at 10:30:10 UTC from IEEE Xplore. Restrictions apply.